JOURNAL OF MATERIALS SCIENCE 33 (1998) 3001–3007

Electrical transport studies and temperature-programmed oxygen evolution of $PrO_{1.83}$

R. G. BISWAS†, M. RAJENDRAN, G. S. WALKER*, E. WILLIAMS, A. K. BHATTACHARYA‡
Centre for Catalytic Systems and Materials Engineering, Department of Engineering, University of Warwick, Coventry, CV4 7AL, UK

The phases in the homologous series Pr_nO_{2n-2} ($n=11$, 10, 9 and 7) have been studied by temperature-programmed reduction (TPR), electrical conductivity and Seebeck coefficient measurements using $PrO_{1.83}$ as the starting material. TPR measurements in helium indicate that oxygen evolution from $PrO_{1.83}$ occurs in three distinct steps and quantification of the oxygen evolution shows the formation of the phases Pr_nO_{2n-2} ($n=10$, 9 and 7). Temperature-dependent electrical conductivity measurements for $p(O_2)=0$ show breaks in the conductivity which occur at 635, 714 and 797 K, whereas in air the breaks occur only at 720 and 953 K. These correspond to the compositionally controlled phase transitions. The Arrhenius conductivity expression has been used to calculate the activation energies and pre-exponential factors in the stoichiometric regions. Results from TPR and conductivity experiments indicate that $PrO_{1.83}$ and $PrO_{1.71}$ have easily established temperature ranges of composition while $PrO_{1.80}$ and $PrO_{1.78}$ have stability ranges which are very much smaller. Seebeck coefficient measurements (thermopower) as a function of oxygen partial pressure and temperature indicate that the conduction changes from n to p type for the composition $PrO_{1.71}$. The approximate independence of the Seebeck coefficient with temperature fits the Heikes theory for a hopping conductor. The discrepancies in the earlier reports on the conductivity of $PrO_{1.83}$ are attributed to the variations in the $p(O_2)$ employed, rate of heating and also to a certain extent the partial hydroxylation and carbonation of the samples used. The results of the present experiments point out these aspects and clarify the discrepancies between previously published data.

1. Introduction

The oxides of praseodymium in the range Pr_2O_3–PrO_2 are able to form a whole series of non-stoichiometric phases and also a homologous series with the generic formula Pr_nO_{2n-2}, with $n = 4$, 7, 9, 10, 11, 12 and ∞. Among these oxides $PrO_{1.833}$, the $n = 12$ member, is the most common obtained by thermally decomposing praseodymium salts. On heating, $PrO_{1.833}$ undergoes a series of compositionally controlled phase transitions [1, 2] dependent on the oxygen partial pressure. The sequence of phase transitions between $n = 12$ and $n = 4$ is of the following order and has the designation sequence given below:

$$PrO_{1.833}(\text{ordered})\ (\beta) \rightarrow PrO_{1.83}(\text{disordered})\ (\beta'(\equiv \alpha)) \rightarrow PrO_{1.818}(\delta) \rightarrow PrO_{1.800}(\varepsilon) \rightarrow PrO_{1.778}(\zeta) \rightarrow PrO_{1.714}(\iota)$$

The stability of a particular phase depends on the experimental parameters such as oxygen partial pressure and temperature; however, the sesquioxide Pr_2O_3 is formed only under reducing conditions. Temperature-dependent vacuum decomposition of $PrO_{1.83}$ [3] showed the phase transitions $PrO_{1.833} \rightarrow PrO_{1.800} \rightarrow PrO_{1.778} \rightarrow PrO_{1.714}$ occurring at temperatures of 663 K, 693 K and 753 K, respectively [3, 4]; however, these data were not quantified and the compositions were assumed by the relevant workers. Also, the rate of heating was not specified in this report which can lead to errors in the temperatures assigned to the formation of the various phases. Thermogravimetric analysis by Eyring and Baenziger [4] on PrO_x ($x \approx 1.83$) also showed the formation of the phases between $n = 4$ and 12 with formation temperatures of 623, 693 and 773 K. Again, these reported temperatures were probably

† *Present address:* 29 Caithness Close, Coventry, West Midlands, UK.
* *Present address:* Department of Materials Engineering and Materials Design, University of Nottingham, University Park, Nottingham NG7 2RD, UK.
‡ To whom all correspondence should be addressed.

dependent on the rate of heating employed in the experiment.

The phase diagrams and structural features for the praseodymium oxide system have been studied in detail by Hyde *et al* [1, 2] and Eyring and Baenziger [4]. The structure of the phases with composition greater than the sesquioxide are fluorite related and may be viewed as the removal of oxygen atoms from normal sites in the fluorite structure accompanied by a relaxation of the remaining atoms proportionate to the extent of oxygen vacancy [4]. The actual crystal structures of these praseodymium oxides are complex and Pr_6O_{11}, for instance, may well be represented by the formula $Pr_{24}O_{44}$.

Electrical transport measurements on the oxides are of interest because of the narrow conduction bandwidths due to the 4f electronic structure and the presence of both Pr^{3+} and Pr^{4+} cations in most of the oxides, allowing electron or hole hopping. Transport measurements such as conductivity [3–12], thermopower [5–7], dielectric constant [8] and magnetic susceptibility [8, 13] have been attempted on some oxides. The first electrical measurements [11] suggested that the oxides higher than $PrO_{1.71}$ were n-type semiconductors. Noddack and Walsh [12] also found very high intrinsic conductivity in PrO_x compared with other rare earths. The first break in the temperature-dependent resistivity of $PrO_{1.833}$ was shown by Eyring and Baenziger [4] and was attributed to the change in stoichiometry of the oxide. Chandrashekar *et al.* [7] measured the temperature-dependent conductivity between 444 and 666 K for $PrO_{1.833}$ and assumed an Arrhenius temperature dependence for the conductivity to calculate an activation energy for conduction. However, our reinterpretation of their data shows that there is an observable break in the conductivity at 645 K and that their data do not fit a single linear temperature dependence over the whole temperature range measured. Lal and Verma [8] have measured the resistivity of $PrO_{1.833}$ in the temperature range 150–800 K and found deviations from linearity at 600 and 700 K which are quite different from the earlier reports [4]. More recent data obtained by Inaba and Naito [9, 10], who made simultaneous measurements of oxygen pressure, composition and electrical conductivity for the phases $n = 10$, 9 and 7, found breaks and hysteresis for every phase change and that there was no conductivity maximum around the [O]/[Pr] ratio of 1.75. However, this study contradicts the earlier findings of Honig *et al.* [5] and Subba Rao *et al.* [6] who performed thermopower measurements at 473 K and 673 K, respectively, and showed that for $[O]/[Pr] > 1.75$ the conduction is n type while for $[O]/[Pr] < 1.75$ the conduction is p type, and that the conductivity is proportional to the product $(x - 15)(2 - x)$ of the concentrations of Pr^{3+} and Pr^{4+} ions where x is the [O]/[Pr] ratio and a maximum in the conductivity exists at [O]/[Pr] of approximately 1.75. Conductivity measurements as a function of oxygen dependence [6] on $PrO_{1.833}$ have shown that over the temperature range 465–384 K the conduction was due to anion vacancies according to the relation

$$O_0^{2-} \longleftrightarrow \tfrac{1}{2}O_2(g) + V_O'' + 2e^- \qquad (1)$$

However, for $[O]/[Pr] < 1.68$ the conduction was due to cation vacancies, confirming that the sign of the charge carriers will be p-type as found from the thermopower data. Analysis by Subba Rao *et al.* [6] and Chandreshekar *et al.* [7] predicted that the charge carriers were small polarons by nature of the closeness of the dimension of the polaron compared with the lattice constant, the narrow conduction bandwidths and the magnitude of the Fröhlich coupling constant. A small polaron is a defect created when an electronic carrier becomes localized owing to the surrounding atoms or ions. Thus, in the rare earth dioxides such as CeO_{2-x}, PrO_{2-x} and TbO_{2-x} the production of a $3+$ valence ion reduces the energy near the O^{2-} ion and the resultant polarization traps the electrons. Small-polaron formation is favourable in materials whose conduction-band electrons belong to partially filled f or d shells and because of the small electron overlap produces narrow conduction bandwidths. Since charge transport of the small polaron involves the movement of the lattice distortion, the mobility of the carrier is low compared with that in broad-band semiconductors which gives a method for determining whether the small polaron is the charge carrier. At high temperatures, this movement is thermally activated and thus the mobility of the charge carriers has an associated activation energy [14, 15].

Some other problems with electrical transport studies of previously published data include an arbitrary conductivity scale [4], non-Arrhenius conductivity plots [8], non four-probe sample geometry [6, 8] and unknown sample environment gas, thus making interpretation of the data difficult. The present study is undertaken to clarify the discrepancies in the published conductivity data and to highlight the phase transitions occurring during the temperature programmed reduction of $PrO_{1.83}$.

2. Experimental methods

2.1. Preparative methods

A sample of $PrO_{1.83}$ ($PrO_{2-\delta}$, $\delta = 0.17$) was produced by heating pure (99.9%) Pr_6O_{11} (Aldrich) to 1473 K for 2 h and by then furnace cooling in synthetic air at a rate of 50 K h^{-1}. The X-ray diffraction pattern was then compared against the standard Joint Committee of Powder Diffraction Standards reference pattern.

2.2. X-ray diffraction

X-ray powder diffraction patterns for samples were recorded in the region $2\theta = 10$–90° with a step scan of 0.1° min^{-1} on a Philips diffractometer (model PW1710) using Cu Kα radiation. Cell parameters were calculated and further refined using linear regression procedures (Philips APD 1700 software) applied to the measured peak positions of all major reflections up to $2\theta = 90^\circ$. Accurate measurement of peak shift was carried out on selected small-angle reflections.

2.3. Temperature-programmed reduction

Temperature programmed reduction (TPR) of the samples under an inert atmosphere was carried out using a flow reactor with the exhaust gases measured using a Hiden quadrupole mass spectrometer. Freshly prepared oxide samples (about 0.2 g) were loaded into a stainless steel reactor tube using quartz wool plugs to position the sample. The temperature of the sample was controlled by a Newtronics Micro96 temperature controller. Helium (cp grade; BOC) was dried by passing through a liquid-nitrogen trap; other gases were used as received. Helium was passed over the sample at a flow rate of 50 ml min^{-1} (atmospheric pressure) and the sample was heated at a rate of 10 K min^{-1} to 1023 K. Loss of oxygen was measured by recording the $m/z = 32$ signal. The mass spectrometer was calibrated after each experiment using a Valco valve to inject 1.0 ml pulses of oxygen (research grade; BOC).

2.4. Electrical characterization

2.4.1. Electrical conductivity

Bar-shaped specimens for electrical conductivity measurements were pressed from the prepared powder into bars of approximately 1.5 mm thickness and sintered at 1473 K for 2 h. Ag paste contacts were then applied to the ends of the pellets. Pt wire loops for potential measurements were then secured along a third of the pellet length with Ag paste. Conductivity measurements were performed using a Keithley 220 constant-current source and Keithley 617 electrometer for voltage measurements using a four-wire measurement configuration. The sample was mounted between spring loaded Pt discs in an alumina sample holder within a temperature-controlled furnace. Two sample currents were used for every temperature measurement point to ensure that the measured resistance was not electric field dependent and all measurements were performed either in a flowing dried oxygen–nitrogen mix ($p(O_2) = 150$ Torr) or in argon atmosphere according to the experimental conditions. Measurements were repeated on other specimens and were found to agree within experimental error. Detailed measurements were performed at 2.5 K intervals with a ramp rate of 30 K h^{-1}.

2.4.2. Seebeck coefficient measurements

Thermoelectric power measurements were performed using the differential method. A disc shaped sample was clamped between Pt discs with a Pt–Rh thermocouple attached to each disc. Five temperature gradients of up to 5 K for each mean sample temperature were produced across the sample using a direct-current (d.c) heater and the thermoelectric voltage measured with respect to the Pt leads using a Keithley 181 nanovoltmeter. Samples were placed in a furnace with all measurements performed under computer control. The Seebeck coefficient or thermopower was calculated from the gradient $\Delta V/\Delta T$ for the five temperature gradients and where the correlation coefficients were higher than 0.97.

3. Results and discussion

The powder X-ray diffraction pattern of the undoped black compound praseodymium oxide shows an excellent match with the published Joint Committee on Powder Diffraction Standards data [16] for the face-centred cubic form of $PrO_{1.83}$ belonging to the space group *Fm*3*m*. The refined lattice parameter of the as-prepared $PrO_{1.83}$ corresponds to $a = 5.470(8)$ Å and is found to be in agreement with the reported value of $a = 5.468$ Å for $PrO_{1.83}$ [4]. Its cell volume of 163.74 $Å^3$ is an excellent match with a value of 163.62 $Å^3$, as reported in the literature.

The loss of oxygen during TPR of $PrO_{1.83}$ under an inert atmosphere is given in Fig. 1 and shows that oxygen was evolved in three distinct temperature regions. A fresh sample of $PrO_{1.83}$ shows the complete absence of peaks for m/e values of 18 and 44, ensuring the complete absence of hydroxyl and carbonate contaminants. The oxygen evolution begins at 633 K with the maximum peaks at 708, 758 and 803 K. The amounts of oxygen associated with the peaks at 708, 758 and 803 K were estimated by calculating the peak areas after background corrections to give 0.0160(0) mol, 0.011(0) mol and 0.032(5) mol, respectively, of oxygen. These correspond to the formation of $PrO_{1.80}$, $PrO_{1.779}$ and $PrO_{1.714}$, respectively. The change in x for PrO_x with temperature is also plotted in Fig. 1 and clearly shows the formation of the three different phases. The calculated values of stoichiometry from the TPR data are in good agreement with the theoretical estimates and the well-known homologous series of phases $PrO_{1.80}$, $PrO_{1.778}$ and $PrO_{1.714}$.

The temperature-dependent electrical conductivities of the sintered $PrO_{1.83}$ pellet in $p(O_2) = 150$ Torr and $p(O_2) = 0$ Torr atmospheres are given in Fig. 2a and b, respectively. Measurements were obtained in the temperature range 273–1000 K, at atmospheric pressures with conductivity values obtained in approximately 25 K increments. The results for $p(O_2) = 150$ Torr (Fig. 2a) indicate that there is a linear

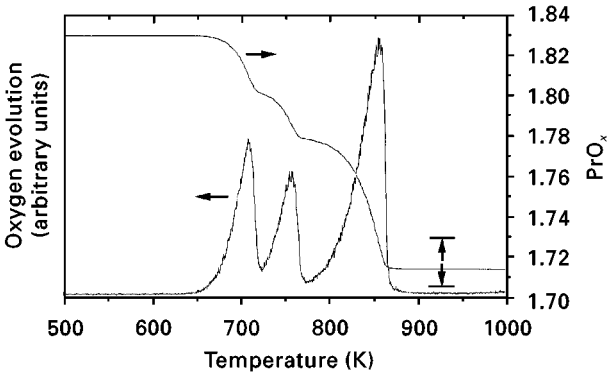

Figure 1 TPR of $PrO_{1.83}$ under helium. Oxygen evolution and the corresponding change in stoichiometry of PrO_x plotted against temperature.

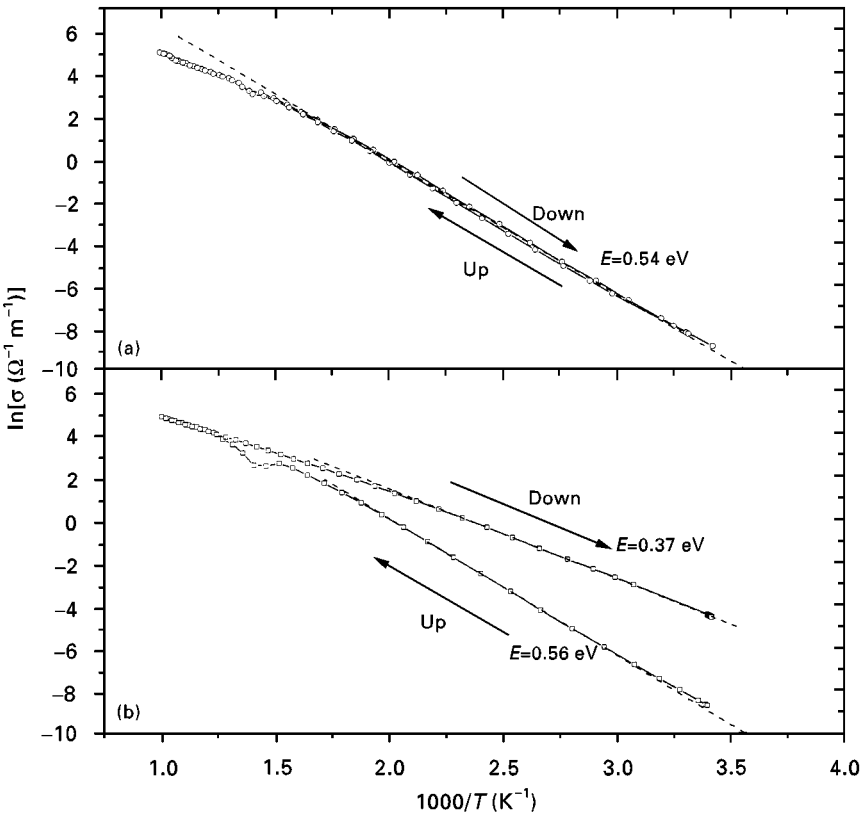

Figure 2 Arrhenius plots of the conductivity variation of $PrO_{1.83}$ (a) at $p(O_2) = 150$ Torr and (b) $p(O_2) = 0$ Torr.

dependence over the temperature range 500– 333 K. Assuming the Arrhenius conductivity expression which may be written as $\sigma_t = A \exp(-E_\sigma/kT)$, where σ_t is the measured conductivity, k is the Boltzmann constant, A is the pre-exponential constant and E_σ is the activation energy for conduction, the activation energy in this temperature range is calculated as $E_\sigma = 0.54$ eV and is lower than the value of 0.81 eV calculated by Chandrashekar *et al.* [7]. At higher temperatures the $\ln \sigma_t$ versus $1000/T$ graph shows two discontinuities: a larger magnitude change at 720 K and a smaller change at 953 K. These probably indicate the phase transformations between β and α and α to ı [1]. Re-examination of the earlier measurements by Chandrashekar *et al.* [7] showed a discontinuity in the temperature-dependent conductivity at 645 K but our results appear to be similar to those of Eyring and Baenziger [4] who found discontinuities at 773 and 925 K, although these workers provided no absolute determination of conductivity. Measurements of the conductivity performed at $p(O_2) = 0$ Torr (Fig. 2b) show a much larger variation in conductivity at 666 K. The calculated activation energies for the temperature run up and run down data between 333 and 500 K are 0.56 eV and 0.37 eV, respectively. Thus, the activation energy between 333 and 500 K at $p(O_2) = 150$ Torr is almost the same as that found at $p(O_2) = 0$ Torr (Fig. 2a). The preparation and storage of the prepared conductivity sample were found to be important as the oxide would absorb water or CO_2 from the atmosphere such that the physical characteristics of the pellet may not remain stable. A small amount of hydroxylation or carbonation of the oxide is below the detection limit of X-ray diffraction or energy-dispersive analysis of X-ray characterization techniques; however, it has been found that it can affect the grain-boundary conductivity [14]. Thus, the total conductivity of the pellet measured by d.c techniques may be slightly in error and will thus give an erroneous activation energy.

A more detailed study of temperature-dependent conductivity of $PrO_{1.83}$ at $p(O_2) = 150$ Torr showed that there was noticeable hysteresis, between the temperature run up and run down data for the transformation at 720 K which is a similar effect to that noticed by Eyring and Baenziger [4]. Fig. 3 shows the temperature-dependent conductivity data obtained at $p(O_2) = 0$ Torr over the temperature range 410–1000 K with more data points collected (every 2.5 K) than for the plot given in Fig. 2b. The data show that there are three transitions and four phases present, confirming the TPR data given in Fig. 1. The linear sections of Fig. 3a, i.e., $T > 816$ K, correspond to the non-stoichiometric limits of the ordered phases which for this temperature range is the ı phase. The curved regions of the graphs are assigned to the two-phase regions. Thus, for temperatures less than 606 K the β phase is stable, between 689 and 721 K the ε phase is stable, between 793 and 741 K the ξ phase is stable and for temperatures above 816 K the ı phase is stable. The data confirm that the phases $PrO_{1.83}$ and $PrO_{1.71}$ have easily established temperature ranges of composition while $PrO_{1.80}$ and $PrO_{1.78}$ have stability ranges which are very much smaller [1].

PrO_x is thought to be a mixed conductor at low temperatures owing to the presence of oxygen

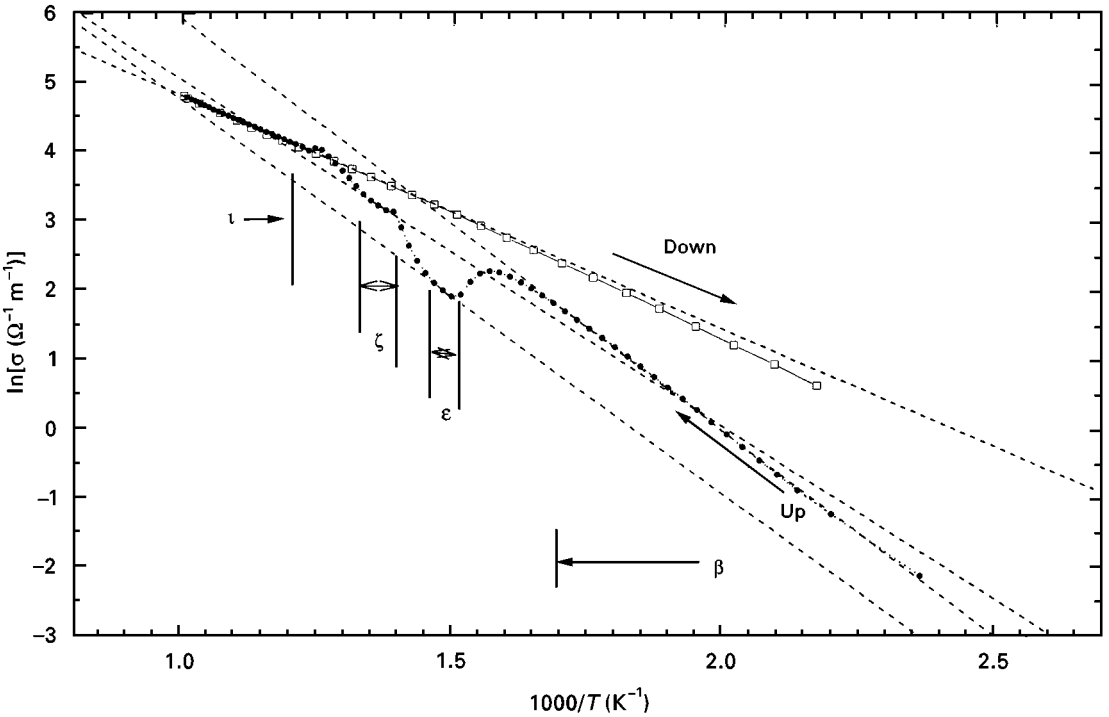

Figure 3 Arrhenius plot of the conductivity variation of $PrO_{1.83}$ at $p(O_2) = 0$ Torr over the temperature range 410–1000 K. (Only every third data point is plotted to aid presentation.)

vacancies and low-mobility small polarons [4]; however, at high temperatures the electronic conductivity via the hopping of holes or electrons will dominate the conductivity. Thus, at high enough temperatures the total conductivity σ_t for PrO_x could be written as [15]

$$\sigma_t = c(1-c)\left(\frac{e^2a^2\nu}{kT}\right)\exp\left(\frac{-E_\sigma}{kT}\right) \qquad (2)$$

where c is the concentration of available hopping sites, $c(1-c)$ is the probability that a jump can take place assuming that the available sites are randomly distributed, a is the lattice constant, and ν is the carrier "jump" vibrational frequency and $-E_\sigma$ is the activation energy for carrier "hopping". Using the data shown in Fig. 3, the activation energies for the conduction in these ordered phases can be determined from the linear portions of the slopes and are given in Table I. The activation energies and pre-exponential factors decrease with decreasing n (Table I), with the lowest activation energy and pre-exponential factor found for $PrO_{1.71}$. The conductivity is also found to increase with decreasing n, with the maximum conductivity found for $PrO_{1.71}$. The activation energy E_σ depends on the order of the oxygen vacancies and distribution of Pr^{3+} ions and suggests that for decreasing n in Pr_nO_{2n-2} the order of the structure increases. This "order" then reduces the energy required for a carrier hop. The number of charge carriers increases as expected for oxygen evolution according to Equation 1 and explains the increase in the conductivity for decreasing n in Pr_nO_{2n-2}.

The Seebeck coefficient has been calculated from the measured electromotive force across the praseodymium between the temperatures of 300 and 1000 K in atmospheres with $p(O_2) = 150$ Torr and $p(O_2) = 0$ Torr and these data are presented in Fig. 4. The sign of the cold end of the sample was used to give an indication of the sign of the carriers and for measurements made at $p(O_2) = 150$ Torr indicates that the conduction is n type up to 1000 K. However, results at $p(O_2) = 0$ Torr indicate that the sign of the carriers are initially n type and changes to p-type conduction at 820 K corresponding to the phases $PrO_{1.83}$ and $PrO_{1.71}$. Data within the temperature range 660–820 K are less reliable and it was not possible to assign accurate values to the stoichiometric ranges $PrO_{1.80}$ and $PrO_{1.78}$. The data confirm the theory that a change from n- to p-type conduction occurs at this $x = 1.75$ value. Since the composition $PrO_{1.75}$ is unstable, the next reduced stable oxide is $PrO_{1.71}$ which is confirmed in our conductivity and TPR data. The Seebeck coefficient data at $p(O_2) = 150$ Torr and $p(O_2) = 0$ Torr up to 600 K are closely related, confirming the observations made from the conductivity data within the same temperature regime.

TABLE I Calculated electrical transport parameters from the temperature-dependent conductivity of PrO_x measured at $p(O_2) = 0$ Torr

Temperature range (K)	E_σ (eV)	A ($\Omega^{-1}\,m^{-1}$)	x in PrO_x	Phase
< 606	0.512	141×10^3	1.83	β
667–679	0.49	34.2×10^3	1.80	ε
714–734	0.43	23.0×10^3	1.78	ξ
> 816	0.29	3.6×10^3	1.71	ι

Conventional broad-band semiconductor theory predicts that the Seebeck coefficient for a single charge

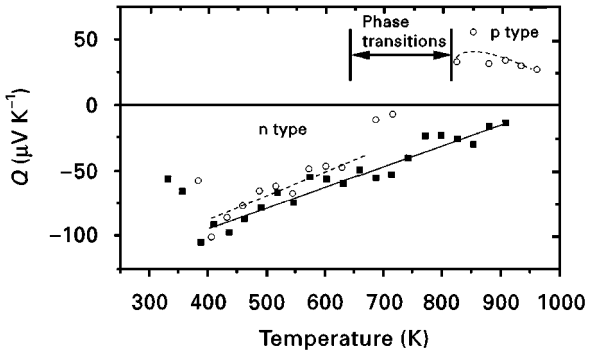

Figure 4 The temperature-dependent Seebeck coefficient of $PrO_{1.83}$ at $p(O_2) = 150$ Torr (○) and $p(O_2) = 0$ Torr (■).

carrier type can be obtained from

$$Q = \pm\frac{k}{e}\left(\frac{E_F}{kT} + A\right) \tag{3}$$

where E_F is the Fermi energy with respect to the conduction band, k is the Boltzmann constant, T is the absolute temperature, e is the electron charge and A is a dimensionless constant dependent on the scattering mechanisms. Equation 3 may be rewritten assuming n-type conduction to give

$$Q = \pm\frac{k}{e}\left[\ln\left(\frac{N}{n}\right) + A\right] \tag{4}$$

where N is the density of states in the conduction band and n is the carrier concentration where for band-type conduction n is found from

$$n = N\exp\left(\frac{-E_F}{kT}\right) \tag{5}$$

Substitution of Equation 5 into Equation 4 shows that the conduction and thermopower energies should be equivalent:

$$\frac{\delta(\ln\sigma)}{\delta(1/T)} = \frac{-Qe/k}{1/T} = \frac{-E_F}{k} \tag{6}$$

A plot of $-Qe/k$ versus $1/T$ allows the thermopower activation energy E_S to be calculated. Analysis of the data in Fig. 4 gives $E_S = 0.05$ eV, and the conductivity activation energy $E_\sigma = 0.55$ eV (Table I). Mott [17] has suggested that the difference between the thermopower and conduction activation energies may be due to a polaron conduction mechanism for a materials system. For a small-polaron conduction mechanism to operate, the charge carriers are localized at specific cation sites and have to move through the materials by hopping which is an activated process so that the mobility of the carriers has an activation energy. Equation 4 is often referred to as the Heikes [18] formula so that Equation 4 can be written as

$$Q = -\frac{k}{e}\left[\ln\left(\beta\frac{1-c}{c}\right) + A\right] \tag{7}$$

where $c = n/N$ where n is the number of electrons, N is the number of available sites and β is the degeneracy factor. The constant A is typically small for metal oxide systems and is generally neglected [19] and $\beta = 1$. Observation of Equation 7 indicates that the thermopower for small-polaron hopping contains no adjustable parameters such as temperature and thus depends only on n and N. Band conduction predicts that the Seebeck coefficient is proportional to $1/T$. Therefore, for a fixed stoichiometry in praseodymium oxide, the Seebeck coefficient should be constant and, for n-type conduction in praseodymium oxide, Equation 7 can be rewritten as

$$Q = -\frac{k}{e}\frac{x - 1.5}{2 - x} \tag{8}$$

Observation of Fig. 4 shows that the Seebeck coefficient is roughly independent of temperature and depends on the value of x only. However, the small temperature dependence may be due to the contribution of ionic conduction as a result of the presence of oxygen vacancies. Thus, the Seebeck coefficient may be written as $Q = (Q_i\sigma_i + Q_e\sigma_e)/\sigma_t$, where the subscripts i an e refer to the ionic and electronic contributions, respectively. At approximately 820 K the Seebeck coefficient changes sign to indicate p-type conduction in $PrO_{1.71}$. To calculate the mobility, μ, of the charge carriers, the well-known expression $\sigma = ne\mu$ may be used, assuming one type of carrier, and the experimentally derived values of electrical conductivity, σ, and carrier concentration, n. Therefore, to calculate the charge carrier concentration, Equation 7 is rearranged to give

$$n = \frac{N}{1 + \exp(-Qe/k)} \tag{9}$$

For low-mobility semiconductors and for exceedingly narrow or localized levels the density of states, N, is approximated as $4 \times 10^{22}\,cm^{-3}$ [20]. Table II shows the calculated values of carrier concentration and mobility at 600 and 800 K for data derived at $p(O_2) = 150$ Torr. The mobility values are of the order previously published and are in the range 10^{-3}–10^{-8} $cm^2\,V^{-1}\,s^{-1}$ expected for oxide semiconductors [19]. The increasing mobility with increasing temperature also confirms that a hopping model rather than a band-type model is responsible for the type of conduction mechanism.

TABLE II Electrical conduction parameters for $PrO_{1.83}$ in air at 600 K and 800 K

T (K)	Q ($\mu V\,K^{-1}$)	σ ($\Omega\,cm^{-1}$)	n (cm^{-3})	μ ($cm^2V^{-1}s^{-1}$)
600	−64	0.049	1.3×10^{22}	2.4×10^{-5}
800	−30	0.425	1.6×10^{22}	1.6×10^{-4}

4. Conclusions

This work has shown for the first time a detailed study of the temperature dependence of the electrical conductivity and thermopower of $PrO_{1.83}$ in different gas oxygen partial pressures and quantified TPR data.

The loss of oxygen during the TPR of $PrO_{1.83}$ under an inert atmosphere showed that oxygen was evolved in three stages beginning at 633 K, the rate of evolution passing through maxima at 708 K, 758 K and 803 K corresponding to the formation of the intermediate stoichiometric phases PrO_x at $x = 1.80$, 1.779 and 1.714. This is the first reported direct measurement of the TPR of $PrO_{1.83}$. The temperature-dependent conductivity of $PrO_{1.83}$ at $p(O_2) = 150$ Torr shows that there are two phase transitions present with transitions occurring at 720 K and 953 K corresponding to the phase transitions from β to α and from α to ι. Detailed measurements of the temperature-dependent conductivity at $p(O_2) = 0$ Torr indicate that the intermediate stoichiometric phases PrO_x at $x = 1.80$, 1.78 and 1.71 are observable with transition temperatures at approximately 635 K, 714 K and 797 K, respectively. The phases $PrO_{1.83}$ and $PrO_{1.71}$ have easily established temperature ranges of composition while $PrO_{1.80}$ and $PrO_{1.78}$ have ranges which are very much smaller. The highest conductivity and lowest activation energy is found for $Pr_{1.71}$ and the activation energy decreases for increasing x in PrO_x. The almost constant Seebeck coefficient with temperature agrees broadly with the Heikes equation for a hopping conduction model. The Seebeck data also confirm the change from n- to p-type conduction during the reduction of $PrO_{1.83}$ to $PrO_{1.71}$. This is expected as $PrO_{1.5}$ is an insulator and $PrO_{1.83}$ is an n-type conductor, and the maximum conductivity occurs for equal concentrations of Pr^{3+} and Pr^{4+} ions. The calculated mobilities at 600 and 800 K are less than 0.1 $cm^2 V^{-1} s^{-1}$ which is also indicative of a localized hopping occurring in the oxide semiconductor.

Acknowledgements

M. Rajendran and G. Walker wish to thank the Engineering and Physical Science Research Council for research fellowships. R. G. Biswas thanks the Centre for Catalytic Systems and Materials Engineering for a post-doctoral research assistantship.

References

1. B. G. HYDE, D. J. M. BEVAN and L. EYRING, *Phil. Trans. R. Soc. A*, **259** (1966) 583
2. *Idem*., "Rare earth research", Vol. 2, edited by K. S. Vorres, (Gordon and Breach, New York, 1964), p. 227
3. A. F. CLIFFORD and P. A. FAETH, "Rare earth research", edited by E. V. Kleber (Macmillan, London, 1961), p. 105.
4. L. EYRING and N. C. BAENZIGER, *J. Appl Phys.* **33** (1962) 209.
5. J. M. HONIG, A. A. CELLA and J. C. CORNWELL, "Rare earth research", Vol. 2, edited by K. S. Vorres, (Gordon and Breach, New York, 1964) p. 555.
6. G. V. SUBBA RAO, S. RAMDAS, P. N. MEHROTRA and C. N. R. RAO, *J. Solid State Chem.* **2** (1970) 377.
7. G. V. CHANDRASHEKAR, P. N. MEHROTRA, G. V. S. RAO, E. C. SUBBA RAO and C. N. R. RAO, *Trans. Faraday Soc.* **63** (1967) 1295.
8. H. B. LAL and B. K. VERMA, *Indian J. Pure Appl. Phys.* **15** (1977) 400.
9. H. INABA and K. NAITO, *J. Solid State Chem.* **50** (1983) 100.
10. *Idem*., *ibid.* **50** (1983) 111.
11. R. I. MARTIN, *Nature*, **165** (1950) 202.
12. W. NODDACK and H. WALSH, *Z. Physik. Chem.* **211** (1959) 194.
13. S. KERN, *J. Chem Phys*, **40** (1964) 208.
14. Unpublished results.
15. T. HOLSTEIN, *Ann. Phys., NY* **8** (1959) 343.
16. Joint Committee of Powder Diffraction Standards, "Powder diffraction file" (International Center for Diffraction Data, Swarthmore, PA), Card 6-329.
17. N. F. MOTT, "Conduction in non-crystalline materials" (Clarendon, Oxford, 2nd Edn, 1993).
18. R. R. HEIKES, "Rare earth research", edited by E. V. Kleber (Macmillan, London, 1961, p. 105.
19. J. B. GOODENOUGH, *Prog. Solid State Chem.* **5** (1974) 145.
20. F. J. MORIN, *Phys. Rev.* **93** (1953) 1195.

Received 13 October 1997
and accepted 3 March 1998